This article has been accepted for publication in a future issue of this journal, but has not been fully edited. Content may change prior to final publication. Citation information: DOI 10.1109/JBHI.2016.2518202, IEEE Journal of Biomedical and Health Informatics

An Algorithm for Real-Time Pulse Waveform Segmentation and Artifact Detection in Photoplethysmograms

Christoph Fischer*, *Member, IEEE*, Benno Dömer, Thomas Wibmer, and Thomas Penzel, *Senior Member, IEEE*

***Abstract*—Photoplethysmography has been used in a wide range of medical devices for measuring oxygen saturation, cardiac output, assessing autonomic function, and detecting peripheral vascular disease. Artifacts can render the photoplethysmogram (PPG) useless. Thus, algorithms capable of identifying artifacts are critically important. However, the published PPG algorithms are limited in algorithm and study design. Therefore, the authors developed a novel embedded algorithm for real-time pulse waveform (PWF) segmentation and artifact detection based on a contour analysis in the time domain. This paper provides an overview about PWF and artifact classifications, presents the developed PWF analysis, and demonstrates the implementation on a 32-bit ARM core microcontroller. The PWF analysis was validated with data records from 63 subjects acquired in a sleep laboratory, ergometry laboratory, and intensive care unit in equal parts. The output of the algorithm was compared with harmonized experts' annotations of the PPG with a total duration of 31.5 hours. The algorithm achieved a beat-to-beat comparison sensitivity of 99.6 %, specificity of 90.5 %, precision of 98.5 %, and accuracy of 98.3 %. The inter-rater agreement expressed as Cohen's kappa coefficient was 0.927 and as F-measure was 0.990. In conclusion, the PWF analysis seems to be a suitable method for PPG signal quality determination, real-time annotation, data compression, and calculation of additional pulse wave metrics such as amplitude, duration, and rise time.**

***Index Terms*—Artifact, contour analysis, decision list, embedded, real-time, pattern recognition, photoplethysmogram (PPG).**

Manuscript received June 17, 2015; revised November 21, 2015; accepted January 07, 2016. Date of publication <month> <day>, <year>; date of current version January 10, 2016. *Asterisk indicates corresponding author.*

This work was supported in part by the German Federal Ministry of Education and Research (BMBF) and in part by MCC GmbH & Co. KG.

*C. Fischer is with Roche Diabetes Care GmbH, Mannheim 68305, Germany, and also with the Department for Cardiology, Interdisciplinary Sleep Medicine Center, Charité Universitätsmedizin Berlin, Berlin 10117, Germany (e-mail: christoph.fischer@ieee.org).

B. Dömer is with MCC GmbH & Co. KG., Karlsruhe 76135, Germany (e-mail: benno.doemer@mcc-med.de).

T. Wibmer is with the Department of Internal Medicine II, University Hospital of Ulm, Ulm 89081, Germany (e-mail: thomas.wibmer@gmx.de).

T. Penzel is with the Department for Cardiology, Interdisciplinary Sleep Medicine Center, Charité Universitätsmedizin Berlin, Berlin 10117, Germany (e-mail: thomas.penzel@charite.de).

Color versions of one or more of the figures in this paper are available online at http://ieeexplore.ieee.org.

Digital Object Identifier <TBD>

I. Introduction

PHOTOPLETHYSMOGRAPHY is a simple optical technology [1], [2]. It uses one or more light emitting diodes to illuminate tissue with differing wavelengths. The intensity of the non-absorbed light at each wavelength is measured by a photodiode. The light absorption and transmission depends on the traveled light path, optical density of the tissue, volume of blood present in the tissue, and blood composition [3]. Two modes of operation exist: 1) transmission mode where the tissue sample is placed between the source and the detector (e.g., fingertip); and 2) reflection mode where the sensor and detector are placed side-by-side (e.g., forehead). Both modes allow a non-invasive measurement of variations of the blood volume over time resulting in a photoplethysmogram (PPG) [4].

A. Pulse Waveform

The PPG consists of a pulsatile (AC) waveform, which is superimposed on a slowly varying (DC) baseline with lower frequency components. The AC component is attributed to cardiac synchronous changes in the blood volume with each heartbeat. The DC component is influenced by respiration, sympathetic nervous system activity, and thermoregulation [5]. The systolic phase starts with a valley that marks the pulse wave begin (PWB) and ends with the pulse wave systolic peak (PWSP). The pulse wave end (PWE) is marked by another valley at the end of the diastolic phase (see Fig. 1). The systolic phase (also called "rise time" in a PPG) varies only in a narrow range inversely proportional to the heart rate compared to the pulse wave duration (PWD) [6], [7]. The narrowing of a single PWD is covered mainly by reduction of the diastolic phase.

Based on the morphology of the diastolic phase five classes of pulse waveforms (PWF)[1] can be distinguished [8]: 1) two distinct notches are inscribed on the downward slope [9], [10]; 2) one distinct notch is inscribed; 3) no notch develops but the line of descent becomes horizontal; 4) no notch is present but a well-defined change in the angle of descent is observed; and 5) no evidence of a notch is seen.

[1] This paper has supplementary downloadable material available at http://ieeexplore.ieee.org, provided by the authors. This includes an overview about performance metrics, pulse wave classifications, and PPG algorithms.

2168-2194 (c) 2015 IEEE. Personal use is permitted, but republication/redistribution requires IEEE permission. See http://www.ieee.org/publications_standards/publications/rights/index.html for more information.

This article has been accepted for publication in a future issue of this journal, but has not been fully edited. Content may change prior to final publication. Citation information: DOI 10.1109/JBHI.2016.2518202, IEEE Journal of Biomedical and Health Informatics

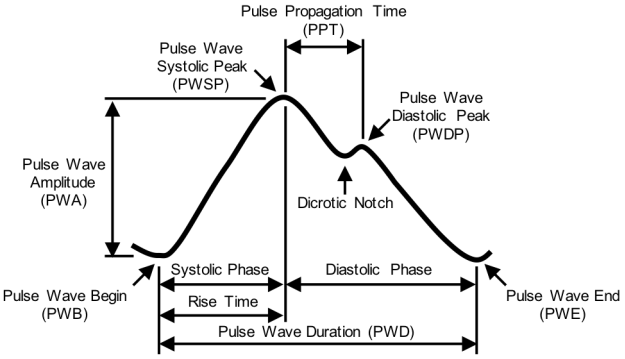

Fig. 1. Pulse Waveform (PWF) of PPG AC part with pulse wave characteristics [5], [13].

B. Artifacts

In general, artifacts can be classified as: 1) technical artifacts (also called experimental errors or technologic); 2) environmental artifacts (also called extrinsic); and 3) biological artifacts (also called physiological artifacts, biologic or intrinsic) [11], [12].

The amplitude and frequency of these artifacts significantly increase when the data collection is moved from the clinic into a patient's home [12]. The development of algorithms capable of removing, or at least identifying, artifacts in the recorded data is therefore critically important [14], [15].

Specifically, motion and noise artifacts are the most common causes of false alarms, loss of signal, and inaccurate measurement in clinical monitoring [16]. They comprise the aforementioned artifact classes and are difficult to filter because they do not have a predetermined frequency band and their spectrum often overlaps with that of the PPG signal [17]. Furthermore, type, incidence, duration, and severity of motion artifacts varied significantly between different environments and patient populations [18].

C. Previous Work

In recent years various algorithms for PWF segmentation and artifact detection in PPG were published. Some of them detect systolic peaks [19]-[23], while others detect in addition the begin of the pulse wave [17], [24]-[28]. There are also algorithms which can detect [17], [21], [22], [25], [29]-[33] or eliminate [34]-[41] artifacts in the PPG.

In addition, some of the mentioned algorithms support a PPG detection even in real-time [17], [20]-[22], [26], [29], [31], [32]. This allows an immediately feedback to the user and can be used to store/transmit/process only the extracted characteristics instead of the complete raw signal.

Processing continuous signals with high resolution requires ample memory and computing power, both of which are limited in a microcontroller. As such, embedded implementations of algorithms that perform well on a PC may not achieve similar results. So far only Farooq et al. [26] and Li et al. [29] published embedded implementations of PPG algorithms on microcontrollers.

In environments with high presence of artifacts or when analyzing single pulse waves, the PPG algorithm should support also beat-to-beat artifact detection. Only the algorithms proposed by Coucerio et al. [25], Karlen et al. [21], Li et al. [30], Orphanidou et al. [23], Robles-Rubio et al. [31], and Sukor et al. [33] provide such detection.

A stable artifact reduction is sometimes more desirable than just artifact detection. However, this requires customized sensors with additional hardware such as ECG [42], MEMS accelerometers [35], or 3rd LED [36] or methods such as time and frequency domain filtering, power spectrum analysis, and blind source separation techniques [34], [37]-[39], [41]. These methods are computationally expensive and more importantly, they also operate on undisturbed signal areas where artifact reduction is not required and could distort the clean signal. Only the method of Salehizadeh et al. [40] affects solely the disturbed area, but it is also computationally expensive because of iterative motion reductions.

For performance tests of ECG detection algorithms there are standards which require the usage of various publicly available databases with recordings from different environments with several subjects [43], [44]. Based on the findings of Tobin et al. [18] it is also important for performance tests of a PPG algorithm to use databases with artifacts varied in type, incidence, duration, and severity from various subjects recorded in different environments. At the moment, no such standard is available for PPG algorithms. The published performance tests of PPG algorithms are heterogeneous with number of subjects from two [19], [27] to 100 [24], duration of pulse waves annotation per subject from 6 seconds [30] to 60 min [19], and limited variety of environments such as only seated rest [20] and rest in supine position [27] to healthy volunteers perform in the field [26].

This literary review shows that to date no algorithm is published that combines real-time detection of PWB, PWSP, PWE and beat-to-beat artifacts, runs on a microcontroller, and is validated with a variety of clinical environments. This prevents the usage in wearable and medically approved recording systems such as next generation of cardiorespiratory polygraph or polysomnograph where onboard signal processing in real-time is desired.

To tackle the problems identified in the previous work, the authors developed a simple real-time PPG analysis with pulse waveform segmentation and artifact detection for various clinical environments. The underlying hypothesis assumes that it is possible to distinguish between reliable and disturbed PPG pulse waves by a time-domain analysis of the PWF morphology. This paper describes the pattern recognition algorithm based on simple filtering techniques and decision lists. It presents also the validation of the algorithm performance with data from various clinical environments. Finally, the embedded firmware implementation on a 32-bit ARM core microcontroller is demonstrated.

2168-2194 (c) 2015 IEEE. Personal use is permitted, but republication/redistribution requires IEEE permission. See http://www.ieee.org/publications_standards/publications/rights/index.html for more information.

This article has been accepted for publication in a future issue of this journal, but has not been fully edited. Content may change prior to final publication. Citation information: DOI 10.1109/JBHI.2016.2518202, IEEE Journal of Biomedical and Health Informatics

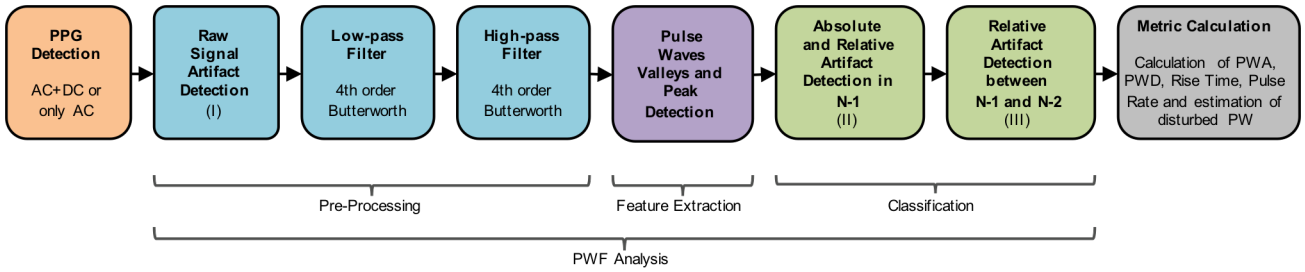

Fig. 2. Flowchart of the PWF analysis with the pattern recognition parts preprocessing, feature extraction and classification. The blocks with artifact detection represent the decision lists (I) to (III). The term N-0 refers to the currently recorded pulse wave, N-1 to the last completely recorded pulse wave and N-2 to the recorded pulse wave before N-1.

II. Materials and Methods

The real-time PPG algorithm performs pattern recognition by analyzing the PWF (see A. Algorithm Description). For development, validation, and referencing of the PWF analysis, databases were built with representative (e.g., sensor applications, walking, body position changes, wake, sleeping) and challenging (e.g., excessive body movements, stress) measurement conditions in clinical environments (see B. Database). To assess the performance of the algorithm records were manually annotated and then a beat-to-beat comparison was performed of the pulse waveform segmentation and artifact detection (see C. Performance Assessment).

A. Algorithm Description

The PWF analysis differentiates artifacts and reliable pulse waves in six stages (see Fig. 2). It is a classification algorithm with three decision lists (see Fig. 3) in the first, fifth and sixth stage [45]. The 13 simple checks of the decision lists monitor several time-domain characteristics of the recording system and pulse waveform in order to detect disturbed pulse waves. For this purpose, pulse wave characteristics were selected, which indicate that a pulse wave is disturbed if the corresponding check fails. As thresholds were used the absolute minimum and/or maximum value of these characteristics found in literature, or if not available taken from the development set (i.e., combination of cohorts Sleep Lab Ulm, Ergometry Lab Ulm, and ICU PhysioBank as shown in Table I), so that no further cohort- or subject-individual training should be required. The basic idea is that each single check is already valid by itself but may only detect a limited number of disturbed pulse waves. With each following check the number of detected disturbed pulse waves increases without incorrect classification of undisturbed pulse waves.

The PWF analysis is called by an application in a loop, which provides the next sample value of the PPG with or without DC part. The first stage with the first decision lists detects clipping values in the raw signal before the proceeding filters alter the signal. The thresholds for top and bottom clipping must be determined only once for each type of recording system because they reflect the signal processing resolutions. These values where derived from the signal channel minimum and maximum.

The power spectrum of the PPG consists of frequency components up to 15 Hz with a dominant power range between 6 and 8 Hz [46], [47]. Therefore, the cutoff frequency of the low-pass filter in the second stage was set to 15 Hz in order to remove higher artifact frequencies (e.g., power line interference).

To suppress the DC part without removing any information about the autonomic nervous system control of the cardiovascular system, the cutoff frequency of the high-pass filter in the third stage was set to 0.01 Hz [47], [48].

After the high-pass filter, the filtered PPG and the raw signal annotation of the PPG are stored in two ring buffers the size of two times the longest permitted duration of a pulse wave, particularly 4.8 s each. The fourth stage then detects potential valleys and peaks of a pulse wave. Therefore, an adaptive threshold is calculated by applying a moving average filter with a span size of 75 % of the last valid PWD. The value 75 % was chosen after a comparison analysis with 50 % and 100 % based on the development set in order to get a threshold, which better tracks DC changes than 100 % without as many false detection of peak candidates in the presence of strong diastolic peaks as compared to 50 %. Then the absolute maximum is identified as potential pulse wave peak in every part of the signal above this threshold, and the absolute minimum is selected as potential pulse wave valley in every signal part below. This allows the detection of potential valleys and peaks even in signals with DC drift (see Fig. 4 mark A). Thereafter, wrongly detected potential peaks and corresponding valleys belonging to diastolic peaks are discarded by demanding that the vertical distance between them multiplied by a factor must be bigger than the previous valid PWA (see Fig. 4 mark B). Based on the development set the factor was set to three. The results of these detections are stored synchronously to the filtered PPG ring buffer in the PPG annotation ring buffer.

Each time a complete pulse wave (called N-1 pulse wave) is recorded, the fifth stage with the second decision list checks absolute and relative pulse wave characteristics. Based on literature-reported values, the permitted range for rise time was set from 0.08 to 0.49 s [6], [49], [50], for systolic-to-diastolic duration ratio (S/D) up to 1.1 [51], [52], for PWD from 0.27 to 2.4 s which corresponds to a pulse rate from 220 to 25 beats per minute (bpm) [53]-[55], and for the number of diastolic peaks up to 2 [9], [10]. The remaining checks in the second decision list are intended to prevent pulse wave detection in a pure noise signal (Check 3) or to detect disturbances of the overall pulse waveform (Check 8 to 10). This artifact annotation is also stored synchronously to the filtered PPG ring buffer in the PPG annotation ring buffer.

2168-2194 (c) 2015 IEEE. Personal use is permitted, but republication/redistribution requires IEEE permission. See http://www.ieee.org/publications_standards/publications/rights/index.html for more information.

This article has been accepted for publication in a future issue of this journal, but has not been fully edited. Content may change prior to final publication. Citation information: DOI 10.1109/JBHI.2016.2518202, IEEE Journal of Biomedical and Health Informatics

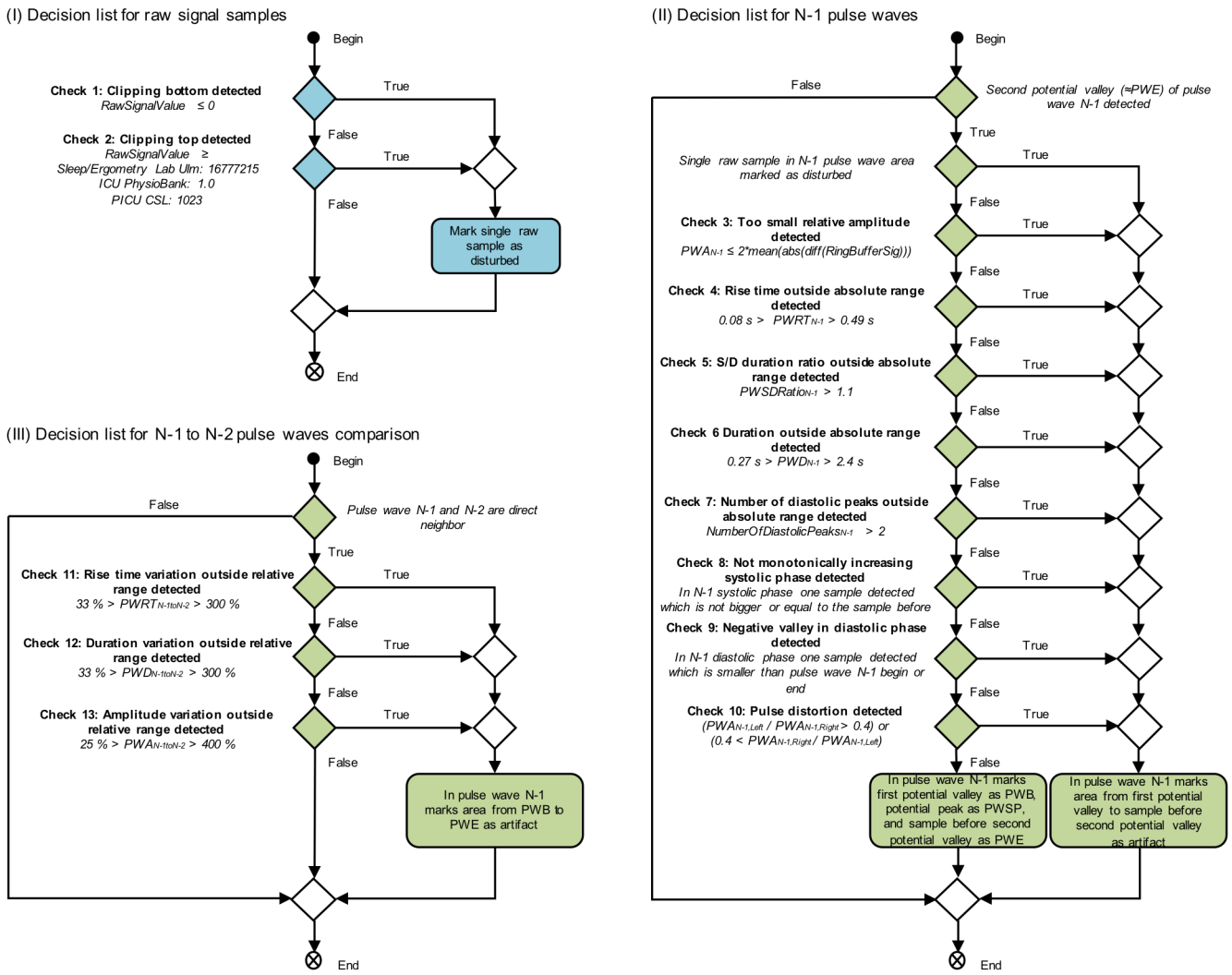

Fig. 3. Activity diagrams of decision lists: (I) raw signal artifact detection per sample value; (II) absolute and relative artifact detection in N-1 per pulse wave; and (III) relative artifact detection between N-1 and N-2 per pulse wave. The term N-0 refers to the currently recorded pulse wave, N-1 to the last completely recorded pulse wave and N-2 to the recorded pulse wave before N-1.

In addition, the sixth stage compares relative changes (Check 11 to 13) of the last complete pulse wave (N-1) with the previous pulse wave (N-2). While the rise time varies in a narrow range with the heart rate according to literature [6], [7], the manually annotated development set shows a beat-to-beat variation from 33 to 300 %. The thresholds for permitted beat-to-beat variation of PWD were set from 33 to 300 % [56] and for PWA from 25 to 400 % [57], as derived from extreme values reported in literature. This artifact annotation is also stored synchronously to the filtered PPG ring buffer in the PPG annotation ring buffer.

The PWF analysis outputs after each processing loop are the filtered PPG value and its annotations delayed by 4.8 s compared to the corresponding input raw PPG sample value.

After the PWF analysis, in a post-processing stage various beat-to-beat metrics like PWA, PWD, rise time and pulse rate are calculated based on the detected pulse waves. Furthermore, the number of pulse waves during artifacts is estimated in order to determine the true negatives for some performance metrics. For that an average PWD based on the mean duration of the undisturbed pulse wave before and after the artifact is fitted into the artifact area.

The PWF analysis was developed in Matlab R2014a (The MathWorks Inc, Natick, USA) with an embedded implementation in mind so that the same functions could be used in Matlab and on a microcontroller. The PWF analysis was also tested in Matlab in a Software-in-the-Loop (SIL) simulation. Afterwards the final PWF analysis was ported from Matlab into ANSI C code and embedded into a small program for data exchange between an Arduino board and a PC. The program was uploaded with Arduino IDE 1.6.1 to an Arduino Due R3-E (Arduino Srl, Scarmagno, Italy). The Arduino Due is a 32-bit microcontroller board based on the Atmel SAM3X8E ARM Cortex-M3 CPU with 512 KB flash memory, 96 KB SRAM and 84 MHz clock speed. In a Processor-in-the-Loop (PIL) simulation, the single sample values of the recorded raw PPG signal were sent via USB from a PC running Matlab to the Arduino board, processed on the microcontroller and then the sample values of the filtered PPG and PPG annotation were sent back to Matlab where the results of the PIL simulation were evaluated and compared with the SIL simulation.

2168-2194 (c) 2015 IEEE. Personal use is permitted, but republication/redistribution requires IEEE permission. See http://www.ieee.org/publications_standards/publications/rights/index.html for more information.

This article has been accepted for publication in a future issue of this journal, but has not been fully edited. Content may change prior to final publication. Citation information: DOI 10.1109/JBHI.2016.2518202, IEEE Journal of Biomedical and Health Informatics

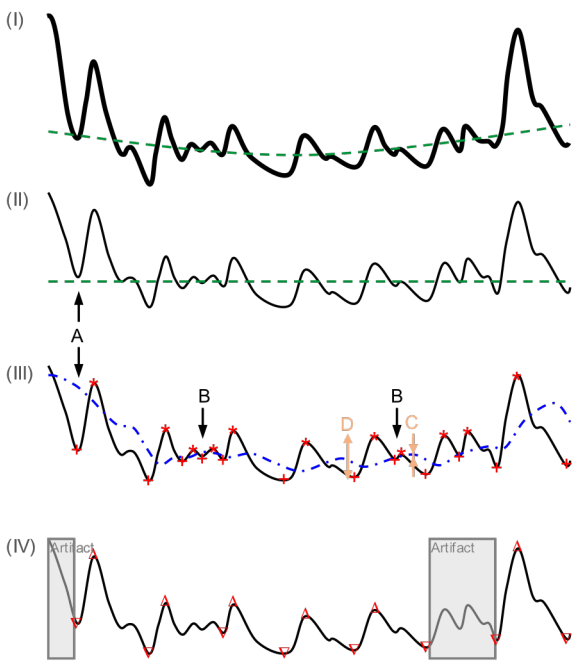

Fig. 4. Illustrated signal decomposition of PWF analysis based on real-life data: I) raw input PPG (–) with high frequency noise and DC (--) drift; II) after pre-processing filtered AC (–) part of PPG and DC at zero line (--); III) after feature extraction calculated adaptive threshold (–·), detected potential valleys (+) and peaks (∗); and IV) after classification output of PWF analysis detected PWB/PWE (∇), PWSP (Δ), and artifacts (□).
Mark A highlights an example for the requirement of an adaptive threshold to identify a potential valley after high-pass filtering in the presence of remaining DC drift.
Mark B highlights examples for the discarding of detected potential peaks and corresponding valleys belonging to diastolic peaks by demanding that the amplitude (C) multiplied by three must be bigger than the previous PWA (D).

B. Database

According to Tobin et al. [18], databases with a broad range of PWF patterns similar to the later algorithm application must be used for validation. In the application area of cardiorespiratory polygraph and polysomnograph, records with PPG from sleep laboratory, ergometry laboratory, and intensive care unit are required. Also raw data with DC part not altered by pre-processing are desired to develop an algorithm, which is independent of algorithms inside the recording device.

None of the three publicly available PPG databases fulfill these requirements. The databases "PhysioBank MIMIC II Waveform Database" with adult intensive care unit records (ICU PhysioBank) [58], [59], "CapnoBase" with recording during general anesthesia [21], [60], and "Complex Systems Laboratory" with pediatric ICU records (PICU CSL) [19] are pre-processed and without DC part. Although "PICU CSL" and "CapnoBase" already provide annotations, the authors had annotated PWSP also in partly disturbed pulse waves. Therefore, the "ICU PhysioBank" database was combined with self-recorded databases from sleep and ergometry laboratory with raw PPG signals including DC part for development and validation (see Table I), whereas the "PICU CSL" was selected as reference because it was already used as such by the authors of "CapnoBase" [21].

Hence, similar to the former benchmark, the two "PICU CSL" records with 60 min each were manually re-annotated with artifacts. The PPG (only AC) was recorded with 10 bits at 125 Hz.

For the "ICU PhysioBank" records the clinical matched subgroup (mimic2wdb-matched) was selected in order to get access to the clinical data. Inclusion criteria were: age of at least 18 years and recording of PPG. About 470 subjects of the database fulfilled the inclusion criteria with a record duration between 803 to 19049 min. The PPG (only AC) were recorded with 10 bits at 125 Hz.

For the "Sleep Lab Ulm" records, 112 subjects referred to the sleep laboratory for PSG (AASM Type 1: full attended polysomnography [61]) were recruited. Inclusion criteria were: age of at least 18 years, suspected or treated sleep apnea, and recording of PPG. Subjects with acute or life-threatening diseases, history of alcohol abuse, or abuse of sedative and hypnotic drugs were excluded. All subjects gave informed consent and the protocol was approved by the local ethics committee (No. 234/11). A standard full-night PSG (SOMNOlab 2 /S, Weinmann Medical Technology, Hamburg, Germany) was applied to all subjects reported to the sleep laboratory. The record duration per subject was between 392 to 510 min. The PPG (with DC and AC) was recorded with 24 bits at 50 Hz.

For the "Ergometry Lab Ulm" records, 24 subjects referred to the ergometer laboratory for ergometry or spiroergometry measurement were recruited. Inclusion criteria were: age of at least 18 years, indication of exercise stress test, and recording of PPG. Subjects with acute or life-threatening diseases of the cardiac system were excluded. All subjects gave informed consent and the protocol was approved by the local ethics committee (No. 346/11). In addition to the clinical routine the same SOMNOlab 2 /S was employed. The record duration per subject was between 30 to 42 min.

The authors are not aware of the existence of guidelines concerning the number of subjects and duration for PPG algorithm validation. Validation sets of former PPG algorithms consisted between 2 to 100 subjects (25^{th}/50^{th}/75^{th} percentile: 9/23/33 subjects) with duration per subject between 6 seconds to 60 min (25^{th}/50^{th}/75^{th} percentile: 0.5/3/10 min) [17], [19]-[21], [23]-[27], [29]-[33]. Thus, from the three databases in total 69 subjects with record durations of 30 min were randomly selected. This on one side exceeds the 75^{th} percentile of number of subjects and duration per subject of former studies and on the other side does not exceed the available "Ergometry Lab Ulm" records so that the three cohorts could be taken equally into account.

Each database was randomly split into approximately 10 % development and 90 % validation records whereby the development set was used for development and literature thresholds verification. Furthermore the development set was used for selection of top/bottom clipping (Check 1 and 2), valid PWA-to-diastolic peak factor (see Fig. 4 mark B) and rise time variation (Check 13) which could not be derived from literature.

2168-2194 (c) 2015 IEEE. Personal use is permitted, but republication/redistribution requires IEEE permission. See http://www.ieee.org/publications_standards/publications/rights/index.html for more information.

This article has been accepted for publication in a future issue of this journal, but has not been fully edited. Content may change prior to final publication. Citation information: DOI 10.1109/JBHI.2016.2518202, IEEE Journal of Biomedical and Health Informatics

TABLE I
SUBJECTS AND MEASUREMENTS CHARACTERISTICS OF THE DEVELOPMENT, VALIDATION AND REFERENCE SET

Parameter	Development set			Validation set			Reference set
	Sleep Lab Ulm	**Ergometry Lab Ulm**	**ICU PhysioBank**	**Sleep Lab Ulm**	**Ergometry Lab Ulm**	**ICU PhysioBank**	**PICU CSL**
Number of subjects	2	2	2	21	21	21	2
Total Cohort Duration in min	60	60	60	630	630	630	120
Sex in male/female	2/0	1/1	1/1	17/4	13/8	13/8	n/a
Age in years	54.5 ± 4.5	54.5 ± 11.5	60.0 ± 10.0	57.1 ± 11.3	61.7 ± 11.4	60.5 ± 15.0	pediatric
BMI in kg/m^2	37.0 ± 10.4	23.2 ± 0.2	n/a	32.1 ± 5.9	28.0 ± 7.4	n/a	n/a
Smoker in never/current/former	1/1/0	1/0/1	n/a	16/5/0	8/2/11	n/a	n/a
Pulse Rate P25 in bpm	57.7	78.9	72.1	60.0	76.9	82.4	111.9
Pulse Rate P50 in bpm	73.2	88.2	78.9	66.7	88.2	91.5	159.6
Pulse Rate P75 in bpm	76.9	100.0	86.2	75.0	100.0	108.7	182.9
Artifact Duration P25 in s	0.8	0.5	0.6	0.9	0.6	0.7	0.5
Artifact Duration P50 in s	1.4	0.7	0.8	1.5	0.8	0.8	0.8
Artifact Duration P75 in s	2.3	1.4	1.5	2.2	1.5	1.5	1.3

Data are presented as mean ± standard deviation and as XXth percentile PXX unless indicated otherwise. The calculation of pulse rate and artifact duration percentiles is based on harmonized experts' annotations.

TABLE II
PULSE WAVES DETECTION PERFORMANCES OF THE DEVELOPMENT, VALIDATION AND REFERENCE SET

Parameter	Development set			Validation set			Reference set
	Sleep Lab Ulm	**Ergometry Lab Ulm**	**ICU PhysioBank**	**Sleep Lab Ulm**	**Ergometry Lab Ulm**	**ICU PhysioBank**	**PICU CSL**
Pulse Waves (TP)	3915	4735	4033	39623	47885	51706	15262
Misclassified Disturbed PW (FP)	24	89	108	379	914	853	78
Misclassified Pulse Waves (FN)	9	14	29	221	175	202	47
Disturbed Pulse Waves (TN)*	142	577	1289	2479	8959	8932	953
Sensitivity (Se) in %	99.8	99.7	99.3	99.4	99.6	99.6	99.7
Specificity (Sp) in %*	85.5	86.6	92.3	86.7	90.7	91.3	92.4
Precision (+P) in %	99.4	98.2	97.4	99.1	98.1	98.4	99.5
Accuracy (Acc) in %*	99.2	97.9	96.7	98.5	97.8	98.0	99.2
Cohen's Kappa coefficient (κ)*	0.892	0.907	0.933	0.885	0.931	0.934	0.934
F-measure (F)	0.996	0.989	0.983	0.992	0.989	0.990	0.996

* The number of disturbed pulse waves (PW) masked by artifacts was estimated using duration of adjacent valid pulse waves.

C. *Performance Assessment*

There is no standardized process available describing how the performance of PPG based detection algorithms should be validated. Following the guidelines proposed by AAMI for ECG based detection algorithms, the sensitivity and precision were calculated to assess the performance of the algorithm [43]. As the PWF analysis detects also artifacts (i.e., true negatives or TN) beside the presence of undisturbed pulse waves (i.e., true positives or TP), specificity and accuracy were calculated. To determine the inter-rater agreement between PWF analysis and harmonized experts' annotations the Cohen's kappa coefficient was calculated [62], which is considered to be an overly conservative measure of agreement [63]. In classification experiments with unknown or undefined number of negative cases, the inter-rater agreement can also be quantified by F-measure [64]. An overview of the used metrics is provided in the supplementary material.

It should be noted that contiguously disturbed pulse waves are indecipherable in most cases because the pulse wave morphology is completely superimposed by the disturbance. The PWF analysis combines them to one artifact (see Fig. 5). Therefore, only an estimated value could be provided for all metrics based on a TN number. The TN number of disturbed pulse waves hidden by an artifact was estimated by simply dividing the artifact duration by a mean PWD based on adjacent valid pulse waves.

To prepare the database for the beat-to-beat comparison, manual annotations for all records were performed by two biomedical engineers with more than nine years of experience in pulse oximetry. One of the biomedical engineers was also involved in the complete study including planning, data collection, developing the Matlab toolbox, developing the PWF analysis, and data evaluation. Alignment meetings between the two engineers were used to score the development set, discuss the algorithm behavior, and define annotation rules. Then both biomedical engineers annotated the remaining datasets without further interactions. For that, the records received the same preprocessing as the PWF analysis. For each single pulse wave the engineers annotated PWB, PWSP, and PWE or artifact. An artifact was defined as a segment in which the signal was substantially disturbed so that: 1) PWB, PWSP, or PWE were not clearly determinable; and/or 2) the morphology of the pulse wave did not correspond to one of the pulse waveform classes (see A. Pulse Waveform). Disagreement was adjudicated by a qualified

2168-2194 (c) 2015 IEEE. Personal use is permitted, but republication/redistribution requires IEEE permission. See http://www.ieee.org/publications_standards/publications/rights/index.html for more information.

This article has been accepted for publication in a future issue of this journal, but has not been fully edited. Content may change prior to final publication. Citation information: DOI 10.1109/JBHI.2016.2518202, IEEE Journal of Biomedical and Health Informatics

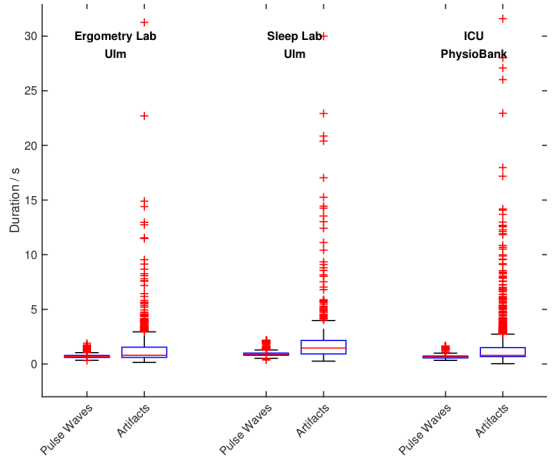

Fig. 5. Boxplot of pulse waves' and artifacts' duration of the validation cohorts based on harmonized experts' annotations limited to duration up to 35 s. In average, the artifacts were larger than the pulse waves because disturbed pulse waves in a row were combined to one artifact.

sleep physician with more than 10 years of experience in pulse wave analysis only knowing the annotation rules. The physician also supervised the data collection in the hospital.

A Matlab toolbox for visualizing and analyzing of biosignal data was developed (see Fig. 6). The toolbox supports the manual annotation by suggesting clipping signal segments, local minimums, and local maximums in user-selectable areas. The beat-to-beat comparison and the calculation of the performance metrics were also implemented in Matlab. In the beat-to-beat comparison between two annotations, pulse waves were considered to match if the time difference between the PWSPs were within an acceptance interval, whereas artifacts considered time differences between begin and duration. The acceptance interval for the development and validation set was one sample difference and for the reference set as in former benchmarks three samples [19], [21].

III. Results

The performance of the PWF analysis was calculated individually for each cohort (see Table II) and combined for the validation set. In total, 139812 undisturbed pulse waves and 22516 estimated disturbed pulse waves were analyzed by the PWF analysis. The detection algorithm identified undisturbed pulse waves with a sensitivity of 99.6 %, leaving 0.4 % of the total number of pulse waves mistakenly annotated as disturbed. Conversely, the PWF analysis mistakenly identified 1.3 % of the disturbed pulse waves as undisturbed. This leads to an overall specificity of 90.5 %, precision of 98.5 %, and accuracy of 98.3 %. The inter-rater agreement based on Cohen's kappa coefficient is 0.927 and based on F-measure is 0.990. In comparison, a local peak finder without proposed checks 1 to 13 has a sensitivity of 99.8 %, specificity of 52.3 %, precision of 94.7 %, accuracy of 94.8 %, Cohen's kappa coefficient of 0.654, and F-measure of 0.972.

The PWF analysis applied to the re-annotated reference set achieved a sensitivity of 99.7 %, specificity of 92.4 %, precision of 99.5 %, accuracy of 99.2 %, Cohen's kappa coefficient of 0.934, and F-measure of 0.996 (see Table II). The CSL algorithm identified 15285 pulse waves, misclassified 757 disturbed pulse waves, and misclassified 24 pulse waves for the same re-annotated reference cohort, which results in a sensitivity of 99.8 %, precision of 95.3 %, and F-measure of 0.975.

The pulse wave characteristics for undisturbed pulse waves observed in the manually annotated development, validation, and reference sets vary within the range of chosen thresholds.

The embedded C code implementation of the PWF analysis in single-precision floating-point format on an Arduino Due requires less than 6.6 KB of the 512 KB Flash memory and for a PPG sampled with 50 Hz less than 3.3 KB of the 96 KB SRAM. The largest part of the SRAM, 1920 Bytes, is used for the two ring buffers (i.e., filtered PPG output and corresponding PPG annotation). The maximal processing time for a single sample value is less then 0.91 ms. The reduction of the signal processing resolution from Matlab (64-bit) to Arduino Due (32-bit) for the given datasets had no effect on the performance, i.e., sensitivity, specificity, precision, and the accuracy were the same for SIL and PIL simulation.

IV. Discussion

The PWF analysis removes artifacts with frequency components above 15 Hz (e.g., power line interference) via proper signal filtering. Remaining artifacts, which disturb the morphology of the pulse waves, are detected and marked. As the discrimination between reliable and disturbed pulse waves is based on 13 threshold checks in the time domain and the storage in ring buffers, the PWF analysis also runs in devices with limited memory capacity and computing power as demonstrated for an Arduino Due. For the given datasets the algorithm works the same in Matlab and Arduino Due because the Matlab implementation was already written like the embedded implementation and the input dataset resolutions of time scale and amplitude were lower than 32-bit. However, it is expected that rounding errors could change the results of single checks when a pulse wave characteristic is near the corresponding threshold value.

In general, algorithm performances could be negatively affected by thresholds derived from a small training set when applied to independent data. Despite the different environments, in the manually annotated validation and reference set the observed pulse wave characteristics varied for all cohorts within the threshold values taken from literature or in the case of valid PWA-to-diastolic peak factor (see Fig. 4 mark B) and rise time variation (Check 13) taken from the development set. This suggests that they are already nearly optimal and further training may not be required. The algorithm can be applied to PPG with different amplitude resolutions, sampling frequencies, and with or without DC part. Only the sampling frequency, bottom (Check 1), and top clipping (Check 2) must be provided for a given recording device. They other parameters are automatically determined (Check 3) or fix (Check 4 to 13).

In literature the distinction between near real-time and real-time is not clearly defined, but implies that there are no significant delays [65]. The design of the presented algorithm discriminates immediately between reliable and disturbed

2168-2194 (c) 2015 IEEE. Personal use is permitted, but republication/redistribution requires IEEE permission. See http://www.ieee.org/publications_standards/publications/rights/index.html for more information.

This article has been accepted for publication in a future issue of this journal, but has not been fully edited. Content may change prior to final publication. Citation information: DOI 10.1109/JBHI.2016.2518202, IEEE Journal of Biomedical and Health Informatics

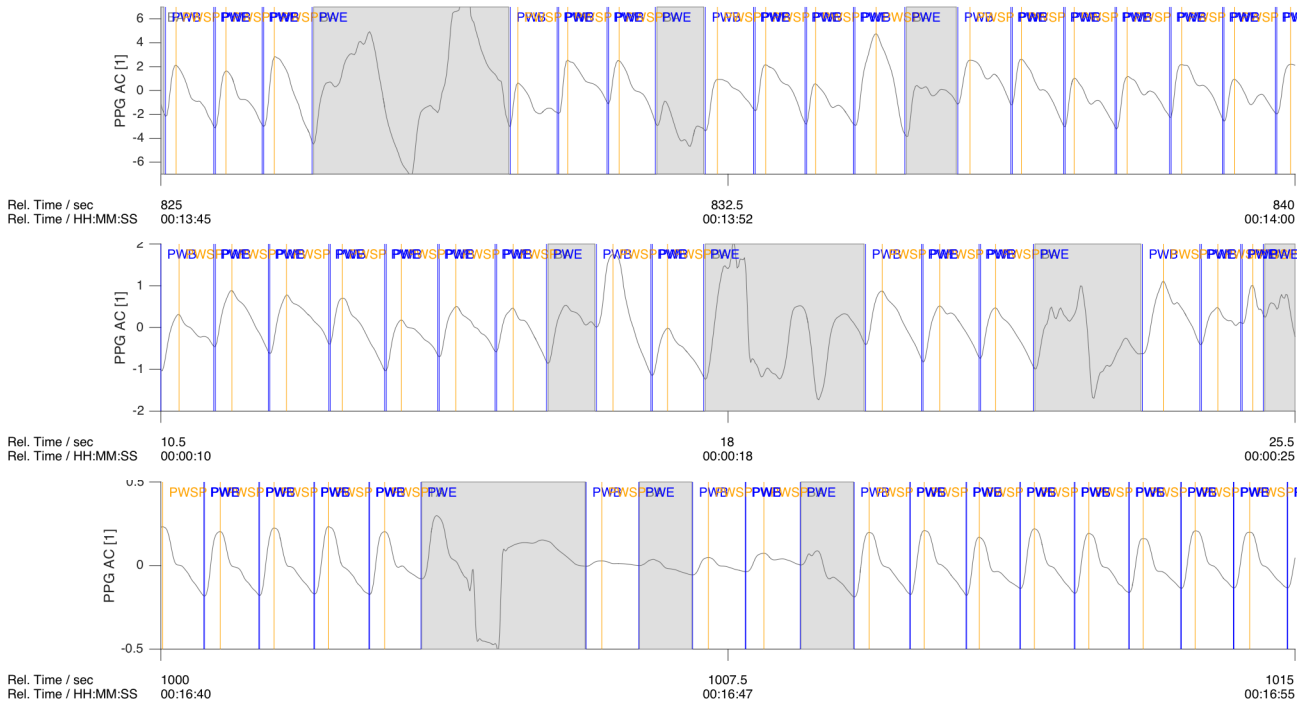

Fig. 6. Examples of the output of the PWF analysis with the AC part of the PPG, pulse waveform segmentations, and artifact annotations taken from a Sleep Lab Ulm (top), Ergometry Lab Ulm (middle), and ICU PhysioBank (bottom) record.

pulse waves following the recording of an undisturbed pulse wave or at most two times the maximal permitted pulse wave duration, which is similar to expert interpretation of such pulse waves. Thus, results of the algorithm are available in real-time according to Shin et al. [66]. The delay of up to 4.8 s does not affect proceeding analyses, if the data is stored with correct time stamps. In most online setups (e.g., sleep laboratory) in which a user views the data on a screen in near real-time, this delay is also negligible as long as the annotations are displayed at the correct position in time.

The algorithm was validated on three cohorts (i.e., Sleep Lab Ulm, Ergometry Lab Ulm, and ICU PhysioBank) combined to one validation set with more than 139800 pulse waves and more than 22500 estimated disturbed pulse waves. The total duration of the validation set exceeds the longest used database with pulse waveform segmentations in literature of 605 min [17] by 1890 min. Only two databases provide larger sample sizes with 100 and 94 subjects, than our validation database with 63 subjects. However, in the database containing 100 subjects, the recorded signals were only 30 s long [24] and from the database with 94 subjects, 132 data segments of 2 min were taken [21].

One reason for the higher percentage of misclassified disturbed pulse waves (i.e., false positives or FP) of 1.3 % compared to misclassified pulse waves (i.e., false negatives or FN) of 0.4 % could be that the algorithm was designed to detect single pulse waves also in disturbed areas. Experts instead tend to reject single pulse waves that are surrounded by artifacts, even if their morphology looks like a valid pulse wave. Accepting a longer delay between input and output, this behavior can be imitated by adding a stage that rejects single pulse waves surrounded by artifacts.

This study is limited by using recorded data containing realistic but uncontrolled disposure of artifacts for validation of the PPG algorithm. In the data records many signal patterns can be found, which indicate the presence of different kinds of artifacts like body movements, power line interference, clipping and others. In most cases it is impossible to determine the cause of artifacts (i.e., technical, environmental, biological, or combination). Furthermore, contiguous disturbed pulse waves are mostly indistinguishable. Therefore, the number of disturbed pulse waves can only be estimated. Simulated data could help to overcome this limitation, but to the authors' knowledge there is no broadly accepted model to simulate PPG signals. Usage of simulated data would lead to new challenges like what is the correct physiological model for PPG simulation, how could the various forms of effects (e.g. arrhythmias, changes of the vasomotoric tone, fluid load changes, body movements) be simulated, how should the effects be superimposed, and reflect these simulations the target environments in the end. Therefore, we decided to use data taken from the target clinical environments.

Another limitation of the study is that a direct performance comparison with other published PPG algorithms is restricted because different validation cohorts and acceptance intervals are used. Applying the various PPG algorithms to the same datasets would eliminate this drawback. But none of them is publicly available and re-engineering would raise other concerns like is the reproduction correct and should the original or optimized parameters for the given environments be used. Only the results of the CSL algorithm [19] are available in a database as annotation. This database was used as reference set. Direct comparison of the PWF analysis with the CSL algorithm shows a slightly lower sensitivity of 99.7 %

2168-2194 (c) 2015 IEEE. Personal use is permitted, but republication/redistribution requires IEEE permission. See http://www.ieee.org/publications_standards/publications/rights/index.html for more information.

This article has been accepted for publication in a future issue of this journal, but has not been fully edited. Content may change prior to final publication. Citation information: DOI 10.1109/JBHI.2016.2518202, IEEE Journal of Biomedical and Health Informatics

versus 99.8 %, better precision of 99.5 % versus 95.3 %, and a better F-measure of 0.996 versus 0.975. In addition, for the validation set a comparison with a local peak finder without proposed checks 1 to 13 is provided showing the improvements in specificity from 52.3 % to 90.5 %, precision from 94.7 % to 98.5 %, accuracy from 94.8 % to 98.3 %, and Cohen's kappa coefficient from 0.654 to 0.927 by only a slightly decreased sensitivity from 99.8 % to 99.6 %.

Apart from these limitations, the PWF analysis is the only published embedded PPG algorithm with PWF segmentation and artifact detection in real-time. An overview of published PPG algorithms is given in the supplementary material.

V. Conclusion

A novel PPG algorithm for pulse waveform segmentation and artifact detection has been proposed. It uses only simple filters and decision lists in order to support a microcontroller implementation. For the first time the authors present an embedded PPG contour analysis, which detects PWB, PWSP, PWE, and beat-to-beat artifacts in real-time. The PWF analysis can be used to:

1) Improve the quality of oxygen saturation and pulse rate calculation in pulse oximeters by ignoring disturbed signal parts.
2) Annotate PPG signals in real-time.
3) Improve the storage and/or data transfer of the PPG by compressing the signal to relevant points of interest (i.e., PWB, PWSP, and PWE). For example, at a pulse rate of 60 bpm and a sampling rate of 50 Hz the data can be reduced from 50 y-values and a fix sample rate to three y- and three x-values. The data compression ratio is then around $51{:}6 \approx 8$ and the space savings are around $(1 - 6/51) \times 100\ \% \approx 88\ \%$.
4) Provide additional pulse wave metrics such as PWA, PWD, and/or rise time.
5) Support the calculation of pulse transit time (PTT) in combination with an ECG detection algorithm.

As a further development the authors would like to add the detection of pulse wave diastolic peaks (PWDP) to support the calculation of pulse propagation time (PPT).

Acknowledgment

The authors would like to thank all participants, who made this study possible. The authors also would like to express their gratitude to the team of MCC GmbH & Co. KG for organizing the study and the helpful feedback, especially K. Pietruska, B. Schöller, and M. Schwaibold. Furthermore, the authors wish to acknowledge the team of the Sleep Laboratory Ulm for performing the data collection, especially B. Schildge, C. Denner, and S. Brunner. A special word of thanks goes to Dr. S. Fischer, N. Hamming, N. Tillery, and Dr. D. Sommermeyer for their helpful feedback on the manuscript.

References

[1] A. B. Hertzman, "The blood supply of various skin areas as estimated by the photoelectric plethysmograph," *Am J Physiol Regul Integr Comp Physiol*, vol. 124, no. 2, pp. 328–340, Oct. 1938.
[2] A. V. Challoner and C. A. Ramsay, "A photoelectric plethysmograph for the measurement of cutaneous blood flow," *Phys Med Biol*, vol. 19, no. 3, pp. 317–328, May 1974.
[3] P. D. Mannheimer, "The light-tissue interaction of pulse oximetry," *Anesth Analg*, vol. 105, no. 6, pp. 10–17, Dec. 2007.
[4] J. Allen and A. Murray, "Similarity in bilateral photoplethysmographic peripheral pulse wave characteristics at the ears, thumbs and toes," *Physiol Meas*, vol. 21, no. 3, pp. 369–377, Aug. 2000.
[5] J. Allen, "Photoplethysmography and its application in clinical physiological measurement," *Physiol Meas*, vol. 28, no. 3, pp. R1–39, Mar. 2007.
[6] A. M. Weissler et al., "Systolic Time Intervals in Heart Failure in Man," *Circulation*, vol. 37, no. 2, pp. 149–159, Feb. 1968.
[7] S. Spitaels et al., "The Influence of Heart Rate and Age on the Systolic and Diastolic Time Intervals in Children," *Circulation*, vol. 49, no. 6, pp. 1107–1115, Jun. 1974.
[8] T. R. Dawber et al., "Characteristics of the dicrotic notch of the arterial pulse wave in coronary heart disease," *Angiology*, vol. 24, no. 4, pp. 244–255, Apr. 1973.
[9] T. Lewis, "The pulsus bisferiens," *Br Med J*, vol. 1, no. 2416, pp. 918–920, Apr. 1907.
[10] W. B. Murray and P. A. Foster, "The peripheral pulse wave: information overlooked," *J Clin Monit*, vol. 12, no. 5, pp. 365–377, Sep. 1996.
[11] D. W. Klass, "The continuing challenge of artifacts in the EEG," *Am J EEG Technol*, vol. 35, pp. 239–269, 1995.
[12] K. T. Sweeney et al., "Artifact removal in physiological signals-Practices and possibilities," *IEEE Trans Inf Technol Biomed*, vol. 16, no. 3, pp. 488–500, May 2012.
[13] M. Elgendi, "Standard Terminologies for Photoplethysmogram Signals," *Curr Cardiol Rev*, vol. 8, no. 3, pp. 215–219, 2012.
[14] M. Chan et al., "Smart wearable systems: current status and future challenges," *Artif Intell Med*, vol. 56, no. 3, pp. 137–156, Nov. 2012.
[15] Y.-L. Zheng et al., "Unobtrusive sensing and wearable devices for health informatics," *IEEE Trans Biomed Eng*, vol. 61, no. 5, pp. 1538–1554, May 2014.
[16] M. T. Petterson et al., "The effect of motion on pulse oximetry and its clinical significance," *Anesth Analg*, vol. 105, no. 6, pp. 78–84, Dec. 2007.
[17] J. W. Chong et al., "Photoplethysmograph signal reconstruction based on a novel hybrid motion artifact detection-reduction approach. Part I: Motion and noise artifact detection," *Ann Biomed Eng*, vol. 42, no. 11, pp. 2238–2250, Nov. 2014.
[18] R. M. Tobin et al., "A characterization of motion affecting pulse oximetry in 350 patients," *Anesth Analg*, vol. 94, no. 1, pp. S54–61, Jan. 2002.
[19] M. Aboy et al., "An automatic beat detection algorithm for pressure signals," *IEEE Trans Biomed Eng*, vol. 52, no. 10, pp. 1662–1670, Oct. 2005.
[20] M. Elgendi et al., "Systolic peak detection in acceleration photoplethysmograms measured from emergency responders in tropical conditions," *PLoS ONE*, vol. 8, no. 10, p. e76585, 2013.
[21] W. Karlen et al., "Adaptive pulse segmentation and artifact detection in photoplethysmography for mobile applications," *Conf Proc IEEE Eng Med Biol Soc*, pp. 3131–3134, 2012.
[22] B. Nenova and I. Iliev, "An automated algorithm for fast pulse wave detection," *Int J Bioautomation*, vol. 14, no. 3, pp. 203–216, 2010.
[23] C. Orphanidou et al., "Signal-quality indices for the electrocardiogram and photoplethysmogram: derivation and applications to wireless monitoring," *IEEE J Biomed Health Inform*, vol. 19, no. 3, pp. 832–838, May 2015.
[24] L. Chen et al., "Automated beat onset and peak detection algorithm for field-collected photoplethysmograms," *Conf Proc IEEE Eng Med Biol Soc*, pp. 5689–5692, 2009.
[25] R. Couceiro et al., "Detection of motion artifacts in photoplethysmographic signals based on time and period domain analysis," *Conf Proc IEEE Eng Med Biol Soc*, pp. 2603–2606, 2012.
[26] U. Farooq et al., "PPG delineator for real-time ubiquitous applications," *Conf Proc IEEE Eng Med Biol Soc*, pp. 4582–4585, 2010.
[27] A. Orjuela-Cañón and H. Posada-Quintero, "Onset and Peak Detection

2168-2194 (c) 2015 IEEE. Personal use is permitted, but republication/redistribution requires IEEE permission. See http://www.ieee.org/publications_standards/publications/rights/index.html for more information.

This article has been accepted for publication in a future issue of this journal, but has not been fully edited. Content may change prior to final publication. Citation information: DOI 10.1109/JBHI.2016.2518202, IEEE Journal of Biomedical and Health Informatics

over Pulse Wave Using Supervised SOM Network," *Int J Biosci Biochem Bioinforma*, vol. 3, no. 2, pp. 133–137, Mar. 2013.
[28] C. Wei et al., "Study on conditioning and feature extraction algorithm of photoplethysmography signal for physiological parameters detection," presented at the 2011 4th International Congress on Image and Signal Processing (CISP), 2011, vol. 4, pp. 2194–2197.
[29] K. Li et al., "Onboard tagging for real-time quality assessment of photoplethysmograms acquired by a wireless reflectance pulse oximeter," *IEEE Trans Biomed Circuits Syst*, vol. 6, no. 1, pp. 54–63, Feb. 2012.
[30] Q. Li and G. D. Clifford, "Dynamic time warping and machine learning for signal quality assessment of pulsatile signals," *Physiol Meas*, vol. 33, no. 9, pp. 1491–1501, Sep. 2012.
[31] C. A. Robles-Rubio et al., "A new movement artifact detector for photoplethysmographic signals," *Conf Proc IEEE Eng Med Biol Soc*, pp. 2295–2299, 2013.
[32] N. Selvaraj et al., "Statistical approach for the detection of motion/noise artifacts in Photoplethysmogram," *Conf Proc IEEE Eng Med Biol Soc*, pp. 4972–4975, 2011.
[33] J. A. Sukor et al., "Signal quality measures for pulse oximetry through waveform morphology analysis," *Physiol Meas*, vol. 32, no. 3, pp. 369–384, Mar. 2011.
[34] R. H. Enríquez et al., "Analysis of the photoplethysmographic signal by means of the decomposition in principal components," *Physiol Meas*, vol. 23, no. 3, pp. N17–N29, Aug. 2002.
[35] P. Gibbs and H. H. Asada, "Reducing motion artifact in wearable bio-sensors using MEMS accelerometers for active noise cancellation," *Proceedings of the 2005, American Control Conference, 2005.*, pp. 1581–1586 vol. 3, 2005.
[36] M. J. Hayes and P. R. Smith, "A new method for pulse oximetry possessing inherent insensitivity to artifact," *IEEE Trans Biomed Eng*, vol. 48, no. 4, pp. 452–461, Apr. 2001.
[37] B. S. Kim and S. K. Yoo, "Motion artifact reduction in photoplethysmography using independent component analysis," *IEEE Trans Biomed Eng*, vol. 53, no. 3, pp. 566–568, Mar. 2006.
[38] M. R. Ram et al., "A Novel Approach for Motion Artifact Reduction in PPG Signals Based on AS-LMS Adaptive Filter," *IEEE Trans Instrum Meas*, vol. 61, no. 5, pp. 1445–1457, May 2012.
[39] T. L. Rusch et al., "Signal processing methods for pulse oximetry," *Comput Biol Med*, vol. 26, no. 2, pp. 143–159, Mar. 1996.
[40] S. M. A. Salehizadeh et al., "Photoplethysmograph signal reconstruction based on a novel motion artifact detection-reduction approach. Part II: Motion and noise artifact removal," *Ann Biomed Eng*, vol. 42, no. 11, pp. 2251–2263, Nov. 2014.
[41] Y.-S. Yan et al., "Reduction of motion artifact in pulse oximetry by smoothed pseudo Wigner-Ville distribution," *J Neuroeng Rehabil*, vol. 2, no. 1, p. 3, Mar. 2005.
[42] C. Yu et al., "A method for automatic identification of reliable heart rates calculated from ECG and PPG waveforms," *J Am Med Inform Assoc*, vol. 13, no. 3, pp. 309–320, May 2006.
[43] "Testing and reporting performance results of cardiac rhythm and ST-segment measurement algorithms," ANSI/AAMI/ISO EC57:1998/(R)2008, 2008.
[44] "Medical electrical equipment - Part 2-27: Particular requirements for the basic safety and essential performance of electrocardiographic monitoring equipment," ANSI/AAMI/IEC 60601-2-27:2011, 2011.
[45] R. L. Rivest, "Learning decision lists," *Mach Learn*, vol. 2, no. 3, pp. 229–246, Nov. 1987.
[46] M. Okada and S. Kimura, "Estimation of arterial pulse wave velocities in the frequency domain: method and clinical considerations," *Med Biol Eng Comput*, vol. 24, no. 3, pp. 255–260, 1986.
[47] A. A. Kamal et al., "Skin photoplethysmography--a review," *Comput Methods Programs Biomed*, vol. 28, no. 4, pp. 257–269, Apr. 1989.
[48] "Heart rate variability: standards of measurement, physiological interpretation and clinical use. Task Force of the European Society of Cardiology and the North American Society of Pacing and Electrophysiology," *Circulation*, vol. 93, no. 5, pp. 1043–1065, Mar. 1996.
[49] D. Golde and L. Burstin, "Systolic Phases of the Cardiac Cycle in Children," *Circulation*, vol. 42, no. 6, pp. 1029–1036, Dec. 1970.
[50] R. P. Lewis et al., "A critical review of the systolic time intervals," *Circulation*, vol. 56, no. 2, pp. 146–158, Aug. 1977.
[51] R. Sarnari et al., "Doppler assessment of the ratio of the systolic to diastolic duration in normal children: relation to heart rate, age and body surface area," *J Am Soc Echocardiogr*, vol. 22, no. 8, pp. 928–932, Aug. 2009.
[52] L. Xiong, "Multi-center pragmatic studies evaluating the time indicator of cardiac perfusion reserve," *JBiSE*, vol. 6, no. 1, pp. 1–7, 2013.
[53] H. Tanaka et al., "Age-predicted maximal heart rate revisited," *J Am Coll Cardiol*, vol. 37, no. 1, pp. 153–156, Jan. 2001.
[54] G. F. G. Fletcher et al., "Exercise standards for testing and training: a statement for healthcare professionals from the American Heart Association," *Circulation*, vol. 104, no. 14, pp. 1694–1740, Oct. 2001.
[55] P. Kligfield et al., "Recommendations for the standardization and interpretation of the electrocardiogram: part I: The electrocardiogram and its technology," *Circulation*, vol. 115, no. 10, pp. 1306–1324, Mar. 2007.
[56] C.-P. Lin et al., "Left Ventricular Systolic Function is Sensitive to Cycle-Length Irregularity in Patients with Atrial Fibrillation and Systolic Dysfunction," *Acta Cardiol Sin*, vol. 28, pp. 103–110, 2012.
[57] A. Rozanski et al., "Peripheral arterial responses to treadmill exercise among healthy subjects and atherosclerotic patients," *Circulation*, vol. 103, no. 16, pp. 2084–2089, Apr. 2001.
[58] M. Saeed et al., "Multiparameter Intelligent Monitoring in Intensive Care II: a public-access intensive care unit database," *Crit Care Med*, vol. 39, no. 5, pp. 952–960, May 2011.
[59] A. L. Goldberger et al., "PhysioBank, PhysioToolkit, and PhysioNet: Components of a new research resource for complex physiologic signals," *Circulation*, vol. 101, no. 23, pp. E215–20, Jun. 2000.
[60] W. Karlen et al., "CapnoBase: Signal database and tools to collect, share and annotate respiratory signals," presented at the Annual Meeting of the Society for Technology in Anesthesia (STA), West Palm Beach, 2010.
[61] C. Iber et al., *The AASM Manual for the Scoring of Sleep and Associated Events*, 1st ed. Westchester, Illinois: American Academy of Sleep Medicine, 2007.
[62] J. Cohen, "A Coefficient of Agreement for Nominal Scales," *Educ Psychol Meas*, vol. 20, no. 1, pp. 37–46, Apr. 1960.
[63] J.-W. Strijbos et al., "Content analysis: What are they talking about?," *Comput Educ*, vol. 46, no. 1, pp. 29–48, Jan. 2006.
[64] G. Hripcsak and A. S. Rothschild, "Agreement, the f-measure, and reliability in information retrieval," *J Am Med Inform Assoc*, vol. 12, no. 3, pp. 296–298, May 2005.
[65] "Telecommunications: Glossary of Telecommunication Terms," Government Institutes, Federal Standard 1037C, Aug. 1996.
[66] K. G. Shin and P. Ramanathan, "Real-time computing: a new discipline of computer science and engineering," *Proc IEEE*, vol. 82, no. 1, pp. 6–24, 1994.

Christoph Fischer (M'06) received the Dipl.-Ing. Degree in electrical engineering and information technology from the Karlsruhe Institute of Technology (KIT), Karlsruhe, Germany in 2005. From 2005 to 2014, he was with Weinmann Medical Technology, Germany. He currently works as Senior Systems Engineer for Roche Diabetes Care GmbH, Mannheim, Germany and is a doctoral student at the interdisciplinary sleep medicine center, Charité University Hospital, Berlin, Germany.

Benno Dömer received the Dipl.-Ing. Degree in electrical engineering and information technology from Aachen University (RWTH), Germany in 2005, and the Dr.-Ing degree from the Karlsruhe Institute of Technology (KIT), Karlsruhe, Germany in 2012. He has been working in the field of sleep diagnosis and photoplethysmography for 9 years and is currently with MCC GmbH & Co. KG, Karlsruhe, Germany.

Thomas Wibmer received the M.D. degree from the University of Munich, Munich, Germany in 2003 and joined the University of Ulm as a research fellow in 2005. He completed a medical residency as well as a fellowship in pulmonology and a fellowship in sleep medicine in 2010, 2012 and 2014, respectively.

Thomas Penzel (M'92–SM'06) received the Graduation degree from physics, human biology, and physiology from the University Marburg, Marburg, Germany, in 1986, 1991, and 1995, respectively. He has been with the University of Marburg since 1984 at the Department of Physics, Physiology, and the sleep laboratory until 2006. Since 2006 he has been the Director of Research of the interdisciplinary sleep medicine center, Charité University Hospital, Berlin, Germany.

2168-2194 (c) 2015 IEEE. Personal use is permitted, but republication/redistribution requires IEEE permission. See http://www.ieee.org/publications_standards/publications/rights/index.html for more information.